Characterization of oxycodone in vitro metabolism by human cytochromes P450 and UDP-glucuronosyltransferases

Romand, Stéphanie Anne; Spaggiari, Dany; Marsousi, Niloufar; Samer, Caroline Flora; Desmeules, Jules Alexandre; Daali, Youssef; Rudaz, Serge

How to cite

ROMAND, Stéphanie Anne et al. Characterization of oxycodone in vitro metabolism by human cytochromes P450 and UDP-glucuronosyltransferases. In: Journal of pharmaceutical and biomedical analysis, 2017, vol. 144, p. 129–137. doi: 10.1016/j.jpba.2016.09.024

This publication URL: https://archive-ouverte.unige.ch/unige:90072
Publication DOI: 10.1016/j.jpba.2016.09.024

Journal of Pharmaceutical and Biomedical Analysis xxx (2016) xxx–xxx

Contents lists available at ScienceDirect

Journal of Pharmaceutical and Biomedical Analysis

journal homepage: www.elsevier.com/locate/jpba

Characterization of oxycodone *in vitro* metabolism by human cytochromes P450 and UDP-glucuronosyltransferases

Stéphanie Romand[a], Dany Spaggiari[a], Niloufar Marsousi[a,b], Caroline Samer[b], Jules Desmeules[b], Youssef Daali[b], Serge Rudaz[a,*]

[a] *School of Pharmaceutical Sciences, University of Geneva, University of Lausanne, Rue Michel Servet 1, 1211 Geneva 4, Switzerland*
[b] *Service of Clinical Pharmacology and Toxicology, Department of Anesthesiology, Pharmacology and Intensive Care, Geneva University Hospitals, 1211 Geneva, Switzerland*

ARTICLE INFO

Article history:
Received 30 June 2016
Received in revised form 6 September 2016
Accepted 24 September 2016
Available online xxx

Keywords:
Oxycodone
Cytochromes P450
UDP-glucuronosyltransferases
In vitro metabolism

ABSTRACT

The hepatic metabolism of oxycodone by cytochromes P450 (CYP) and the UDP-glucuronosyltransferases (UGT), the main metabolic enzymes of phase I and phase II, respectively, was assessed *in vitro*. The *N*-demethylation by CYP3A4/5 and the *O*-demethylation by CYP2D6 in human liver microsomes (HLM) followed Michaelis-Menten kinetics, with intrinsic clearances of 1.46 μL/min/mg and 0.35 μL/min/mg, respectively. Although noroxycodone and oxymorphone mainly contribute to the elimination of oxycodone, the simulated total *in vivo* clearance using *in vitro* phase I metabolism was underestimated. For the first time, metabolism of oxycodone by UGT was deeply investigated using HLM, recombinant enzymes and selective inhibitors. Oxycodone-glucuronide was mainly produced by UGT2B7 (K_m = 762 ± 153 μM, V_{max} = 344 ± 20 peak area/min/mg) and to a lesser extent by UGT2B4 (K_m = 2454 ± 497 μM, V_{max} = 201 ± 19 peak area/min/mg). Finally, the kinetics of the drug–drug interactions were assessed using two CYP and UGT cocktail approaches. Incubations of HLM with phase I and phase II drug probes showed that oxycodone mainly decreased the *in vitro* activities of CYP2D6, CYP3A4/5, UGT1A3, UGT1A6 and UGT2B subfamily with an important impact on UGT2B7.

1. Introduction

Oxycodone (4,5-epoxy-14-hydroxy-3-methoxy-17-methylmorphinan-6-one) is a semisynthetic opioid that acts as an agonist of the μ and κ receptors in the central nervous system [1]. This drug is used to treat moderate to severe pain [2]. Oxycodone is extensively metabolized and bioactivated by hepatic cytochromes P450 (CYP), and less than 10% of the dose is excreted in urine in its unchanged form [3]. Generally, phenanthrene opioids undergo conjugative metabolism by uridine diphosphate (UDP) glucuronosyltransferases (UGT) in the liver and are excreted in urine [4,5]. A small amount of oxycodone was shown to be excreted as conjugated form by analyzing human urine before and after treatment with β-glucuronidase [6,7]. Although CYP-dependent metabolism of oxycodone is well established, the involvement of UGT in biotransformation is currently unclear. The main phase I metabolite, noroxycodone (Fig. 1), is produced by *N*-demethylation at position 17 by CYP3A4/5, whereas the *O*-demethylation of oxycodone into oxymorphone is catalyzed by CYP2D6 [8,9]. The active *O*-demethylated metabolite is 14 times more potent than oxycodone and its affinity for the μ-opioid receptor is 3- to 5-fold higher than morphine [10]. In contrast to morphinan derivatives, oxycodone possesses a methyl group at the 3-position and a keto group at the 6-position, making the hydroxyl group attached to carbon 14 the only position available for *O*-glucuronidation. To date, no data about the *in vitro* glucuronidation of oxycodone by human liver microsomes (HLM) or recombinant UGTs are available. The involvement of different metabolic pathways in the biotransformation of oxycodone could potentially generate clinically meaningful changes in the drug pharmacokinetics (PK), leading to adverse effects or reduced analgesia [11]. Currently, more comprehensive estimations of the magnitude of pharmacokinetic changes are made possible by using a physiologically based pharmacokinetic (PBPK) model, in which drug, body and trial components interact with each other in the same dynamic *in silico* model [11]. In the so-called *bottom-up* strategy, predictions

* Corresponding author.
E-mail address: serge.rudaz@unige.ch (S. Rudaz).

http://dx.doi.org/10.1016/j.jpba.2016.09.024
0731-7085/

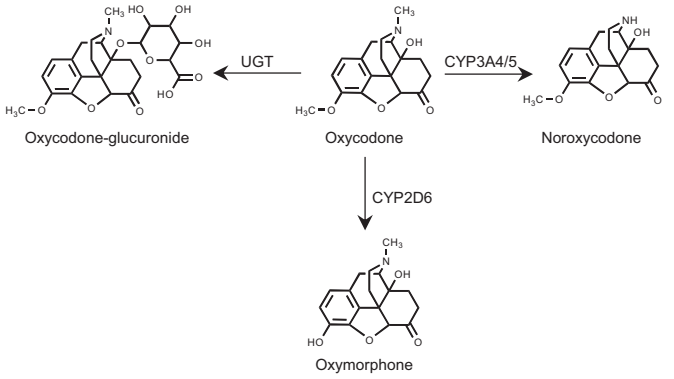

Fig. 1. Metabolic pathways of oxycodone.

are obtained by integrating the drug molecular descriptors and *in vitro* PK parameters in the model [12].

The aim of this study was to characterize the *in vitro* metabolism of oxycodone by the two major drug-metabolizing enzymes pathways, phase I (CYPs) and phase II (UGTs), using ultra-high performance liquid chromatography–mass spectrometry (UHPLC–MS). The UGT isoforms responsible for oxycodone glucuronidation were identified using recombinant UGTs. Inhibition of the formation of phase I and phase II metabolites using CYP-selective and UGT-selective inhibitors was also studied to confirm the isozymes involved in oxycodone metabolism. Finally, the inhibitory effect of oxycodone on the microsomal CYP and UGT isoforms was assessed using two distinct cocktail approaches to evaluate the potential risk of drug–drug interactions involving this compound.

2. Materials and methods

2.1. Chemicals

Oxymorphone, oxymorphone-d3, noroxycodone, noroxycodone-d3, buproprion hydrochloride, dextromethorphan hydrobromide, phenacetin, flurbiprofen, coumarin, etoposide, chenodeoxycholic acid, isoferulic acid, azidothymidine, trifluoperazine dihydrochloride, serotonin hydrochloride, testosterone, fluconazole, naloxone, uridine diphosphate-glucuronic acid (UDPGA), fluoxetine hydrochloride, quinidine anhydrous, ketoconazole, potassium hydroxide, 4-(2-hydroxyethyl) piperazine-1-ethanesulfonic acid sodium salt (HEPES), dimethylsulfoxide, and ammonium hydroxide were provided by Sigma-Aldrich (Steinheim, Germany). Oxycodone hydrochloride monohydrate, codeine hydrochloride, *d*,l-4-hydroxy-3-methoxymethamphetamine hydrochloride, venlafaxine hydrochloride and midazolam were obtained from Lipomed AG (Arlesheim, Switzerland). Levemedetomidine and chlorzoxazone were supplied by Toronto Research Chemicals Inc. (Toronto, Canada). (*S*)-mephenytoin was obtained from Enzo Life Sciences (Lausen, Switzerland). Formic acid was purchased from Merck (Darmstadt, Germany), whereas leucine-enkephalin was obtained from Bachem (Bubendorf, Switzerland). Reduced β-nicotinamide adenine dinucleotide 2′-phosphate tetrasodium salt (NADPH) was provided by Applichem (Darmstadt, Germany). Acetonitrile (ACN) and methanol of ULC–MS grade were obtained from Biosolve (Valkenswaard, Netherlands). Pooled human liver microsomes (HLM) from 20 donors, UGT Supersomes from baculovirus-infected insect cells and reaction mixture-Solution B (250 mM TRIS*HCl, 40 mM $MgCl_2$, 0.125 mg/mL alamethicin and 1.25% (v/v) methanol in water) were purchased from Corning (Amsterdam, The Netherlands). Ultra-pure water was supplied by a Milli-Q purification unit from Millipore (Belfort, NY, USA).

2.2. Solutions

Stock solutions were prepared at different concentrations in water (oxycodone, serotonin, trifluoperazine, azidothymidine, naloxone, fluconazole, NADPH, UDPGA), in methanol (oxymorphone, oxymorphone-d3, noroxycodone, noroxycodone-d3, codeine, *d*,l-4-hydroxy-3-methoxymethamphetamine, chenodeoxycholic acid, levomedetomidine, venlafaxine, fluoxetine, ketoconazole, quinidine, phenacetin, coumarin, bupropion, flurbiprofen, (*S*)-mephenytoin, dextromethorphan, chlorzoxazone and midazolam) or in dimethylsulfoxide (etoposide, testosterone, isoferulic acid). Intermediate concentrations and working solutions were prepared according to the reports of Spaggiari or Gradinaru for phase I and phase II protocols, respectively [13,14].

2.3. Incubation procedures for CYP450- and UGT-dependent metabolism

For experiments regarding the formation of oxymorphone and noroxycodone, HLM (0.5 mg protein/mL) were incubated in a reaction medium containing oxycodone, NADPH and HEPES (pH 7.4, 50 mM) buffer solution. The buffer was prepared by dissolving the required amount of HEPES in water and the pH was adjusted to 7.4 with potassium hydroxide. The final incubation volume was 100 μL and the final concentration of the organic solvent (methanol) was less than 0.5% (v/v). After a 3 min preincubation at 37 °C, the reaction was initiated by adding 2 mM NADPH. The incubation proceeded for 20 min at 37 °C under agitation (400 rpm). The enzymatic reaction was stopped by adding 100 μL of ice-cold ACN containing oxymorphone-d3 and noroxycodone-d3 (final concentration 500 ng/mL). The precipitated proteins were removed by centrifugation (5 min at 10,000 rpm) and an aliquot of the resulting supernatant was transferred to a vial for UHPLC–MS analysis.

Regarding the glucuronidation of oxycodone, HLM or recombinant UGTs (0.5 mg protein/mL) were mixed with the incubation medium containing TRIS*HCl buffer (50 mM, pH 7.5), alamethicin (25 μg/mL) and $MgCl_2$ (8 mM), with the final concentrations given in brackets. After 10 min on ice, oxycodone was added and preincubated for 10 min at 37 °C under agitation (400 rpm). The reaction was then initiated by adding the UDPGA cofactor (4 mM) to a total volume of 100 μL. The final concentration of the organic solvent was less than 0.5% (v/v). The incubation proceeded for 80 min at 37 °C under agitation (400 rpm) and was stopped by adding 100 μL of ice-cold ACN to the reaction medium. The precipitated proteins were removed by centrifugation (10,000 rpm for 10 min) and the supernatant was transferred to a vial for UHPLC–MS analysis.

Each experiment was performed in duplicate or triplicate, and blank reactions were performed in the absence of NADPH or UDPGA. The formation of oxymorphone, noroxycodone and oxycodone-glucuronide was linear with respect to the selected protein concentration and incubation times.

2.4. UGT mapping for oxycodone metabolism

In vitro screening of ten UGT Supersomes (1A1, 1A3, 1A4, 1A6, 1A9, 2B4, 2B7, 2B10, 2B15, and 2B17) that were individually incubated with oxycodone was performed to identify the isoforms involved in its glucuronidation. Incubations with oxycodone (0.5 mM) were performed according to the glucuronidation procedure described in Section 2.3.

Please cite this article in press as: S. Romand, et al., Characterization of oxycodone *in vitro* metabolism by human cytochromes P450 and UDP-glucuronosyltransferases, J. Pharm. Biomed. Anal. (2016), http://dx.doi.org/10.1016/j.jpba.2016.09.024

2.5. Kinetic analysis of oxymorphone, noroxycodone and oxycodone-glucuronide production

Enzymatic kinetics were studied by measuring the formation of the major phase I metabolites in HLM, with oxycodone concentrations ranging from 30 to 1500 μM, as described above. The kinetic parameters for oxycodone glucuronidation in HLM and with recombinant UGT2B4 and UGT2B7 were determined with substrate concentrations ranging from 250 to 6000 μM.

2.6. Targeted inhibition of oxymorphone, noroxycodone and oxycodone-glucuronide production

Targeted inhibition of oxymorphone and noroxycodone production in HLM using a CYP3A subfamily-selective inhibitor (0.3 μM ketoconazole) and CYP2D6-selective inhibitors (10 μM), *i.e.*, quinidine (strong), fluoxetine (medium) and venlafaxine (weak) was assessed by incubating oxycodone at 700 μM. The inhibitory effects of fluconazole (500 and 2500 μM) and naloxone (500 and 1000 μM) on oxycodone (2000 μM) glucuronidation were assessed using HLM and recombinant UGT2B4 and UGT2B7. Control incubations (100% of the control activity) were performed in the absence of inhibitors.

2.7. Assessment of the inhibitory effect of oxycodone using the cocktail approaches

The cocktail approach used to elucidate the impact of oxycodone on the CYP probe reactions was performed as described in the authors' previous work [14]. Briefly, each incubation mixture (100 μL) contained 0.5 mg protein/mL of pooled HLM, HEPES buffer solution (pH 7.4, 50 mM), 2 mM NADPH and eight probe substrates for the major hepatic CYPs. The CYP probe substrates and their final concentrations in the incubation were: phenacetin (CYP1A2, 50 μM), coumarin (CYP2A6, 5 μM), bupropion (CYP2B6, 5 μM), flurbiprofen (CYP2C9, 5 μM), (*S*)-mephenytoin (CYP2C19, 100 μM), dextromethorphan (CYP2D6, 5 μM), chlorzoxazone (CYP2E1, 40 μM) and midazolam (CYP3A4/5, 2.5 μM). Oxycodone was added to the incubation mixture to obtain two distinct final concentrations (300 and 700 μM). The control incubation did not contain oxycodone. After a 3 min preincubation at 37 °C, the CYP450-dependent phase I reactions were initiated by adding 2 mM NADPH. The incubation took place during 20 min at 37 °C under agitation (400 rpm). The enzymatic reaction was stopped by adding 100 μL of ice-cold ACN to the reaction medium. The precipitated proteins were removed by centrifugation (5 min at 10,000 rpm) and an aliquot (150 μL) of the resulting supernatant was transferred to a vial for analysis. Duplicate incubations were conducted.

The inhibitory properties of oxycodone on ten UGT isoforms were simultaneously assessed using a previously described cocktail approach [13]. Briefly, two different concentrations (500 and 1000 μM) of the drug were incubated with HLM and a cocktail of ten specific substrates for the main hepatic UGTs. These substrates and their final concentrations in the reaction medium were: etoposide (UGT1A1, 50 μM), chenodeoxycholic acid (UGT1A3, 14 μM), trifluoperazine (UGT1A4, 5 μM), serotonin (UGT1A6, 100 μM), isoferulic acid (UGT1A9, 50 μM), codeine (UGT2B4/2B7, 50 μM), azidothymidine (UGT2B7, 50 μM), levomedetomidine (UGT2B10, 2 μM), *d*,l-4-hydroxy-3-methoxymethamphetamine (UGT2B15, 35 μM) and testosterone (UGT2B17, 2 μM). The incubation procedure was the same as previously described, with an incubation time of 45 min. After sample centrifugation, the supernatant was evaporated to dryness and the residue was reconstituted after a two-fold preconcentration step in ACN/water (1:9 v/v). Control incubations (100% of the control activity) were performed in the absence of oxycodone, and all incubations were performed in duplicate.

2.8. Instrumentation

2.8.1. Quantitative analysis of oxymorphone and noroxycodone production by UHPLC–MS

The Acquity UPLC system (Waters, Milford, MA, USA) was employed for the chromatographic analyses. The equipment includes a binary solvent manager, an autosampler with a 2 μL loop operating in full loop injection mode, a column manager and a column oven set to 30 °C. The UPLC system was coupled in an optimized configuration with a Xevo® QTOF mass spectrometer (Waters, Milford, MA, USA) fitted with a Z-spray electrospray ionization (ESI) source. The MS operating conditions were set as follows: the desolvation gas (N_2) flow was 1000 L/h (500 °C), the source temperature was 150 °C, the cone gas (N_2) flow was 20 L/h, the collision gas (argon) flow was 0.2 mL/min, and the capillary voltage was 3.0 kV in positive mode. The cone voltage and the extraction cone voltage were 25 V and 4.1 V, respectively. The micro-channel plates (MCPs) were operated at 2200 V with a 4 GHz time-to-digital converter. The QTOF-MS system was operated in the wide-pass quadrupole mode with a low collision energy set to 4 eV to acquire the MS data. Precursor ions were collected in the V-optics centroid mode over an *m*/*z* range of 100–1000 for both functions, with an accumulation time of 0.4 s. The analyses were acquired using programmed dynamic range enhancement (pDRE) technology and an independent reference lock-mass ion infused through the LockSpray™ interface to ensure accuracy and to decrease acquisition variability. A solution of 0.2 μg/mL leucine-enkephalin (*m*/*z* 556.2771) in ACN/water (1:1 v/v) + 0.1% formic acid was used as the reference compound and was infused at a flow rate of 5 μL/min. The LockSpray frequency was set to 20 s (scan duration of 1 s) and was averaged over five spectra. The monitored exact masses for oxycodone, oxymorphone, oxymorphone-d3, noroxycodone, and noroxycodone-d3 were *m*/*z* 316.1549, 302.1392, 305.1581, 302.1392 and 305.1581, respectively. Data acquisition, data handling and instrument control were performed by the Masslynx v. 4.1 software (Waters).

Reversed phase liquid chromatography (RPLC) separations were performed using a Waters Acquity UPLC® HSS-T3 column (50 × 2.1 mm, 1.7 μm) with a flow rate of 500 μL/min with an injection volume of 2 μL. Gradient elution (A: water with 0.1% formic acid; B: ACN with 0.1% formic acid) was used as follows: 2–7% solvent B in 2 min, 7–11.5% solvent B in 3 min, up to 80% solvent B in 0.1 min, and held at 80% solvent B to 5.6 min, followed by column reconditioning at 2% solvent B to 7 min (total analysis time). The retention times for oxycodone, noroxycodone/noroxycodone-d3 and oxymorphone/oxymorphone-d3 were 3.45, 3.28 and 1.60 min, respectively.

For the quantification of the phase I metabolites, calibration samples were prepared by spiking reference standard solutions of oxymorphone and noroxycodone into a mixture of microsomal matrix and stopped with ice-cold ACN containing oxymorphone-d3 and noroxycodone-d3 as internal standards (final concentration 200 ng/mL). Depending on the expected extent of metabolite production, ten concentration levels (500-fold range) were selected for each analytical batch. Samples in tubes were centrifuged and the supernatant was directly injected into the column to assess the oxymorphone and noroxycodone concentrations in the reaction incubation samples using the calibration curves (conventional least-squared linear regression).

2.8.2. UHPLC–MS analysis for the CYP cocktail samples

The LC–MS instrumentation used here was identical to that described above. The same MS parameters were applied, except for

Please cite this article in press as: S. Romand, et al., Characterization of oxycodone *in vitro* metabolism by human cytochromes P450 and UDP-glucuronosyltransferases, J. Pharm. Biomed. Anal. (2016), http://dx.doi.org/10.1016/j.jpba.2016.09.024

the cone voltage, which was set to 30 V in both positive and negative modes. The LC separations were performed on a 100 × 2.1 mm Waters XBridge™ BEH C_{18} XP column with a 2.5 μm particle size and a flow rate of 400 μL/min in the gradient mode (A: water with 0.1% formic acid; B: ACN with 0.1% formic acid, 2–75% B in 15 min, up to 95% B in 0.2 min, held at 95% B to 0.5 min, and then column reconditioning at 2% B to 18 min), with the first 0.5 min diverted to waste. More details about the LC–MS settings are reported in the methods presented in the previous study [14].

2.8.3. UHPLC–MS for the oxycodone-glucuronide and UGT cocktail analysis

The Acquity UPLC system from Waters was equipped with a binary solvent delivery pump, an autosampler with a 2 μL loop operating in full loop injection mode, and a column oven. The UHPLC system was hyphenated with a TQD triple quadrupole mass spectrometer (Waters) fitted with a Z-spray ESI source. The experiments were performed in ESI positive mode with selected reaction mode (SRM). The source temperature, cone gas (N_2) flow and source extractor voltage were 130 °C, 20 L/h and 3 V, respectively. The desolvation gas (N_2) temperature and flow were 450 °C and 1000 L/h, respectively. The capillary voltage was +3000 V. The mass transitions were m/z 316 → 241 for oxycodone (cone voltage: 20 V; collision energy: 10 eV) and m/z 492 → 298 for oxycodone-glucuronide (cone voltage: 30 V; collision energy: 20 eV). Data acquisition, data handling and instrument control were performed by the Masslynx v. 4.1 software.

The LC separations were performed at 25 °C on a Waters Acquity UPLC® BEH C18 column (100 × 2.1 mm, 1.7 μm) with an injection volume of 2 μL and a flow rate of 0.4 mL/min. Oxycodone and its glucuronide were separated using ammonium formate buffer (pH 9.5, 20 mM) (phase A) and ACN (phase B) as the mobile phase. The buffer was prepared with an adequate volume of ammonium hydroxide solution (28% m/v) and adjusted to pH 9.5 with formic acid. The gradient profile was 2–58% phase B in 7 min. The column was re-equilibrated for 4 min at the initial gradient conditions.

2.8.4. UHPLC–MS analysis for the UGT cocktail samples

For the analysis of the cocktail of UGT substrates, the same LC–MS instrument described above was employed with the same operating conditions for MS, including detection in both positive and negative modes (capillary voltages: +3000 V/−3000 V). The mass transitions, cone voltages and collision energies are described in the authors' previous work [15]. The LC separations were performed on a Waters Acquity UPLC® BEH C18 column (100 × 2.1 mm, 1.7 μm) at 25 °C with an injection volume of 2 μL and a flow rate of 0.4 mL/min. The mobile phase consisted of solution A (water + 0.1% formic acid) and solution B (ACN + 0.1% formic acid). The gradient was 2–66% solution B in 7 min. The column was reconditioned for 4 min at 2% solution B.

2.9. Data treatment

The kinetic constants for oxycodone oxidative microsomal metabolism and glucuronidation by HLM and the recombinant UGTs were obtained by fitting the experimental data to the Michaelis-Menten equation (Eq. (1)) using GraphPad Prism (version 5.01; GraphPad software Inc., San Diego, CA, USA).

$$v = \frac{V_{max} \times [S]}{K_m + [S]} \quad (1)$$

where v is the velocity of the reaction (pmol/min/mg for major phase I metabolites and peak area/min/mg for oxycodone-glucuronide), K_m is the Michaelis-Menten constant (μM), V_{max} is the maximal velocity and [S] is the substrate concentration (μM). Intrinsic clearance CL_{int} (μL/min/mg for major phase I metabolites, but no unit for oxycodone-glucuronide) was determined from the ratio V_{max}/K_m.

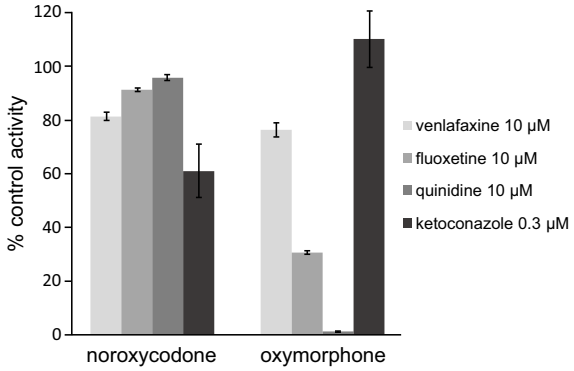

Fig. 2. Inhibition of noroxycodone and oxymorphone production in HLM by venlafaxine (10 μM), fluoxetine (10 μM), quinidine (10 μM) and ketoconazole (0.3 μM). Oxycodone (700 μM) was incubated with the mixture for 80 min at 37 °C. Each bar represents the mean (±range) of duplicate determinations.

The results for targeted inhibitions studies using selective CYP and UGT inhibitors were obtained by expressing the metabolite peak area in the presence of the inhibitor as percentages of the metabolite peak area obtained in the control incubations (100% of control activity). The results from duplicate incubations are presented as the mean (±range).

Activity levels for the drug-metabolizing enzymes (CYP and UGT) obtained using cocktail approaches were expressed as percentages and assessed by dividing the metabolic ratio (specific metabolite to probe substrate peak area ratio) obtained in the presence of oxycodone with the average of duplicate values of the metabolic ratios obtained in the control samples (without oxycodone). The resulting CYPs and UGTs profiles were represented on octagonal and decagonal radar plots, respectively. Each axis represents the relative CYP or UGT activity and the total area of both the octagon and decagon corresponds to 100% of the enzymatic activities.

2.10. PBPK model for oxycodone

PBPK model for oxycodone was developed in 10 healthy male volunteers following the administration of a single dose of oxycodone 0.2 mg/kg using the SimCYP® Population-based ADME Simulator (version 12.0 Simcyp Limited). More details about the model building and refining are reported in a previous paper [11]. The input parameters are given in Table S1 of the Supplementary material.

3. Results and discussion

3.1. Targeted inhibition of noroxycodone and oxymorphone production in HLM

Previous studies have reported that oxycodone *N*-demethylation and *O*-demethylation were catalyzed by CYP3A4/5 and CYP2D6, respectively [8,9]. Inhibition studies performed with selective CYP3A subfamily and 2D6 inhibitors confirmed the contribution of these enzymes to microsomal oxidation of oxycodone, as shown in the results presented in Fig. 2. Indeed, ketococonazole (CYP3A subfamily inhibitor [16]) substantially reduced noroxycodone production (61% of the control activity), but had no impact on oxymorphone production. Venlafaxine, fluoxetine and quinidine are weak [17], medium [18] and strong [9] inhibitors of CYP2D6, respectively. They were used to confirm the contribution of this isoform to oxycodone *O*-demethylation. Accordingly,

Please cite this article in press as: S. Romand, et al., Characterization of oxycodone *in vitro* metabolism by human cytochromes P450 and UDP-glucuronosyltransferases, J. Pharm. Biomed. Anal. (2016), http://dx.doi.org/10.1016/j.jpba.2016.09.024

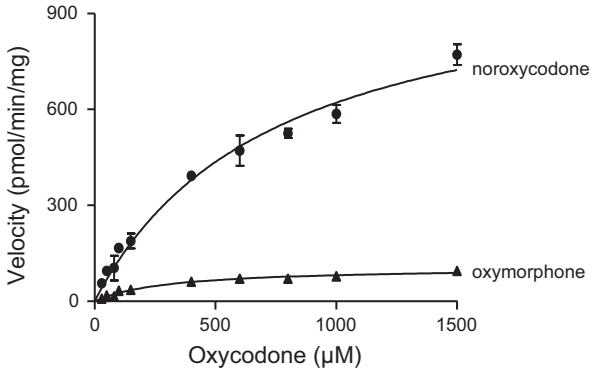

Fig. 3. Michaelis-Menten representations of oxymorphone and noroxycodone production in HLM. Oxycodone (30–1500 μM) was incubated with HLM (0.5 mg protein/mL) for 20 min at 37 °C. The data are the means (±SD) of three independent experiments.

Table 1
Kinetic constants (±CI95%) for oxymorphone and noroxycodone formation by human liver microsomes.

	K_m (μM)	V_{max} (pmol/min/mg)	CL_{int} (μL/min/mg)
oxymorphone	307 ± 95	107 ± 11	0.35
noroxycodone	742 ± 230	1082 ± 161	1.46

Kinetic parameters were calculated by the Michaelis-Menten equation (Eq. (1)).

oxymorphone production decreased as the inhibitor potency increased, but only a weak or negligible effect on noroxycodone production was observed.

3.2. *Kinetic analysis of oxymorphone and noroxycodone formation by HLM* in vitro *for integration into the bottom-up PBPK model*

Oxymorphone and noroxycodone were produced in pooled HLM according to the Michaelis-Menten model (Fig. 3) and the resulting kinetic parameters are presented in Table 1. Oxycodone *N*-demethylation was mediated by a higher affinity catalytic site (lower K_m) and displayed higher velocity value than oxycodone *O*-demethylation in HLM. The intrinsic clearance CL_{int}, which describes *inter alia* the efficiency of the reaction, was higher for noroxycodone formation than for oxymorphone formation (1.46 and 0.35 μL/min/mg, respectively). These results were consistent with a previously reported kinetic analysis of five liver microsomal preparations [8] and were used to simulate the plasma concentration-time profiles of oxycodone after the administration of a single dose of oxycodone 0.2 mg/kg to 10 healthy male volunteers using the existing PBPK model developed by Marsousi et al. (Fig. 4) [11,19]. Based on the results of the targeted inhibition study, the CL_{int} for noroxycodone and CL_{int} for oxymorphone were established as being exclusively mediated by CYP3A and CYP2D6, respectively. The first simulation (Fig. 4A) showed that the total clearance of oxycodone predicted using the *in vitro* phase I-related CL_{int} was underestimated. By including an additional clearance (CL_{add}) using the "parameter estimation" function in the software (see Table S1), the oxycodone profile was clearly predicted better (Fig. 4B). As reported in the literature, glucuronidation was shown to be the second most important metabolic pathway for the clearance of clinically used drugs [20], particularly for phenanthrene opioids. To date, the biotransformation of oxycodone by UGTs was not clearly demonstrated, in contrast to other phenanthrene opioid drugs (for instance, morphine, codeine, and levorphanol). For this reason, oxycodone glucuronidation was studied *in vitro* to evaluate its contribution to the additional clearance required to refine the PBPK model.

3.3. *Glucuronidation of oxycodone by HLM and recombinant UGTs*

RPLC has been broadly used for glucuronides analyses [21–24] and particularly for highly lipophilic stationary phases such as octadecyl-bonded phases C_{18} [25–28]. More recently, RPLC, hydrophilic interaction liquid chromatography (HILIC), aqueous normal phase chromatography (ANPC), and subcritical fluid chromatography (SFC) were compared for their abilities to analyze UGT substrates and their corresponding glucuroconjugates [15]. This study confirmed that an overall better separation quality and better peak shapes were obtained with the stationary phases employed in RPLC and HILIC than those employed in SFC and ANPC. An acidic mobile phase is generally recommended to increase the retention of polar glucuronides (pK_a of approximately 3) through hydrophobic interactions. However, a basic mobile phase was preferred to obtain sufficient selectivity towards oxycodone and its glucuronide for further quantification. Indeed, the tertiary amine functions of oxycodone (pK_a = 7.6 [29]) and its metabolite (pK_a = 7.2 [29]) are neutral at pH 9.5, whereas the glucuronide moiety of the metabolite is fully ionized (pK_a = 2.8 [29]).

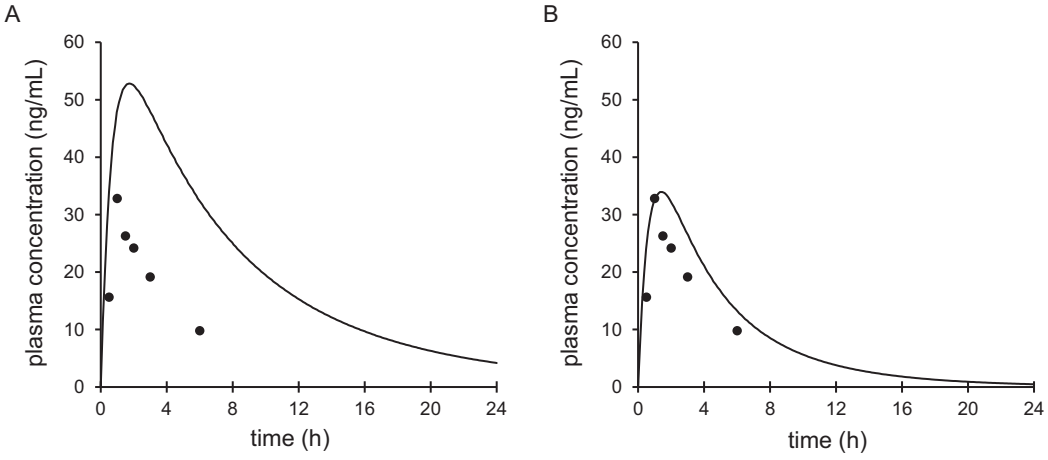

Fig. 4. Observed and simulated concentration-time profile of oxycodone after administration of a 0.2 mg/kg single-dose oxycodone to 10 healthy volunteers. The circles represent the mean concentrations observed by Samer et al. [19], and the solid lines represent the mean concentration profiles for simulated trial using refined parameters (A) without and (B) with additional clearance.

Please cite this article in press as: S. Romand, et al., Characterization of oxycodone *in vitro* metabolism by human cytochromes P450 and UDP-glucuronosyltransferases, J. Pharm. Biomed. Anal. (2016), http://dx.doi.org/10.1016/j.jpba.2016.09.024

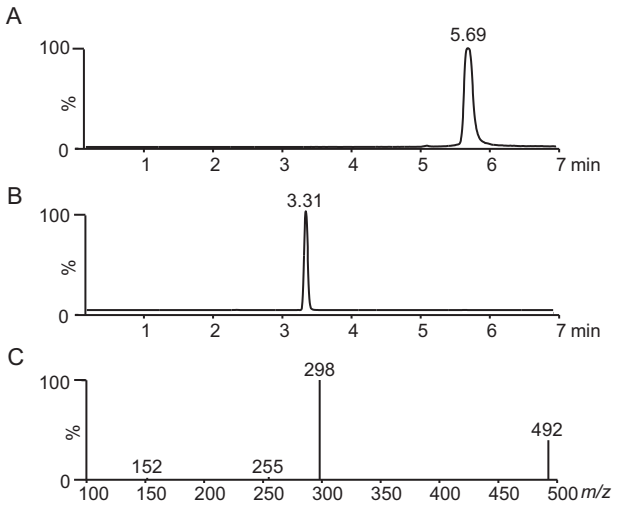

Fig. 5. LC–MS/MS analysis of oxycodone glucuronidation by HLM. Chromatograms of (A) oxycodone (5.69 min) and (B) its glucuronide (3.31 min). (C) Product ion spectrum of oxycodone-glucuronide (*m*/*z* 492).

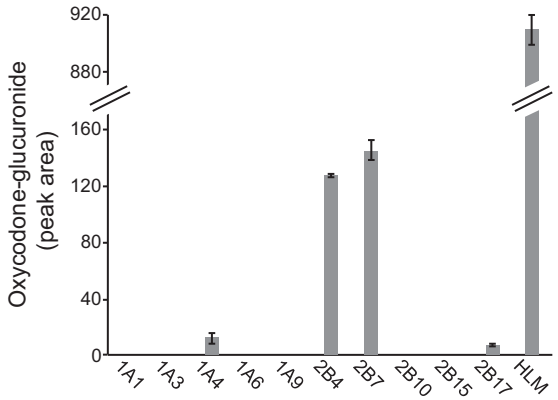

Fig. 6. Oxycodone glucuronidation by recombinant UGTs and HLM. Oxycodone (500 μM) was incubated with each enzyme (0.5 mg protein/mL) for 80 min at 37 °C. Each bar represents the mean (±range) of duplicate determinations.

The UHPLC–MS/MS analysis of the incubation mixture containing HLM, UDPGA and oxycodone showed the presence of two compounds, *i.e.*, the drug and its glucuronide. Indeed, oxycodone (*m*/*z* 316) was eluted at 5.69 min (Fig. 5A), as confirmed by the analysis of a standard solution, whereas the signal *m*/*z* 492 corresponding to the $[M+H]^+$ ion for oxycodone-glucuronide exhibited a peak at 3.31 min (Fig. 5B). For the latter, as a result of simultaneous MS/MS acquisition, the product ion spectrum (Fig. 5C) showed an ion at *m*/*z* 298 corresponding to the loss of the glucuronic acid (molecular weight of 194 Da). The *m*/*z* 492 compound was not observed when oxycodone was incubated without the UDPGA cofactor. This peak confirms the identity of oxycodone-glucuronide, considering that no glucuronide standard was available.

Ten recombinant UGTs were screened to identify which isoforms were responsible for oxycodone glucuronidation. As presented in Fig. 6, UGT2B7 mainly glucuronidated oxycodone, followed by UGT2B4, whereas isoforms 1A4 and 2B17 played a minor role. No detectable glucuronidation activity was observed for UGTs 1A1, 1A3, 1A6, 1A9, 2B10 and 2B15. The involvement of UGT2B7 is not surprising because this enzyme is responsible for the conjugation of numerous drugs, including opioids [30–32]. However, compared to phenanthrene opioids, which are glucuronidated at the 3-OH and/or 6-OH positions, oxycodone only possesses a hydroxyl group at carbon 14. A previous study postulated that

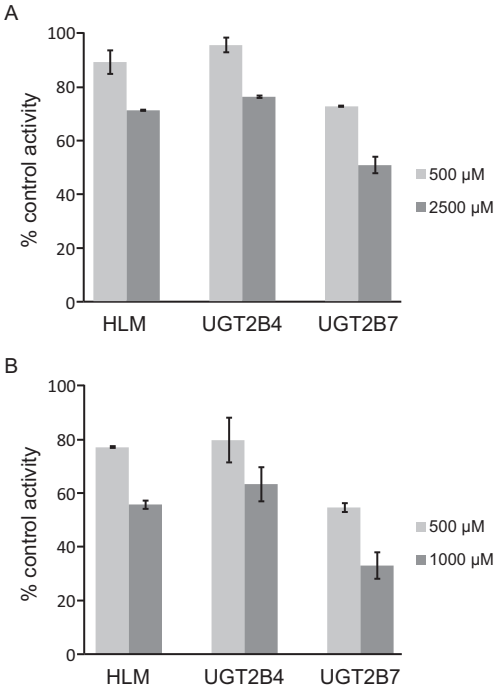

Fig. 7. (A) Fluconazole and (B) naloxone inhibited oxycodone glucuronidation by HLM and the recombinant UGTs 2B4 and 2B7. Oxycodone (2000 μM) was incubated with each enzyme (0.5 mg protein/mL) for 80 min at 37 °C. Each bar represents the mean (±range) of duplicate determinations.

oxycodone glucuronidation was prevented because of the good stability and the poor accessibility of the 14-OH group in the ring structure composed of five carbons and one nitrogen atom [33].

3.4. Inhibition of oxycodone glucuronidation in HLM and recombinant UGTs

Inhibition studies with fluconazole and naloxone were performed with HLM and the recombinant UGTs 2B4 and 2B7 to validate the results from the UGT screening. Fluconazole is known to be a selective inhibitor of UGT2B7 (IC50 = 2500 μM) [34], but an inhibitory effect on UGT2B4 has also been reported [35]. Naloxone is almost exclusively metabolized by UGT2B7 [36,37] and was used as a probe substrate for competitive inhibition studies [38–40]. The inhibitory effect of fluconazole and naloxone on oxycodone glucuronidation activities in HLM, UGT2B4 and UGT2B7 are shown in Fig. 7A and B, respectively. At 500 μM, fluconazole and naloxone barely inhibited HLM and UGT2B4 activities, whereas UGT2B7 activity was more affected (72% and 54% of the control activity with fluconazole and naloxone, respectively).

At higher concentrations, oxycodone-glucuronide production by UGT2B7 was substantially decreased (50% and 33% of the control activity for fluconazole and naloxone, respectively) and to a lesser extent for HLM and UGT2B4. These results confirm that isoforms 2B4 and 2B7 were both involved in oxycodone glucuronidation.

3.5. Kinetic analysis of oxycodone glucuronidation by HLM and recombinant UGT2B4 and UGT2B7

Because UGT2B4 and UGT2B7 represented the main isoforms responsible for oxycodone glucuronidation, kinetic studies were performed with HLM and recombinant UGT2B4 and UGT2B7. As shown in Fig. 8, all data were best fitted by the Michaelis-Menten model and the resulting parameters are presented in Table 2. The 2B7 isoform was more active than 2B4, with V_{max}/K_m values of

Please cite this article in press as: S. Romand, et al., Characterization of oxycodone *in vitro* metabolism by human cytochromes P450 and UDP-glucuronosyltransferases, J. Pharm. Biomed. Anal. (2016), http://dx.doi.org/10.1016/j.jpba.2016.09.024

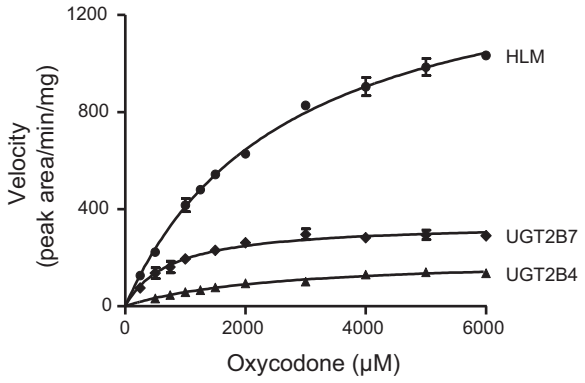

Fig. 8. Michaelis-Menten representations of oxycodone glucuronidation by HLM, UGT2B4 and UGT2B7. Oxycodone (250–6000 μM) was incubated with HLM or the recombinant UGTs (0.5 mg protein/mL) for 80 min at 37 °C. The data are the means (± SD) of three independent experiments.

0.45 and 0.08, respectively. UGT2B7 also showed a higher affinity for oxycodone (K_m values of 762 and 2454 μM for UGT2B7 and UGT2B4, respectively). By comparing the HLM results with those from the recombinant UGTs, the K_m values for HLM and UGT2B4 were similar, whereas the V_{max} value for HLM was 4- to 8-fold higher than the values obtained for the recombinant UGTs. Considering the very low rates of glucuronidation, this metabolite was not quantified. These results confirm the similar recovery of oxycodone in human urine before and after enzymatic or acidic hydrolysis reported elsewhere [3,33,41–43]. Consequently, the additional clearance required to adjust the observed and predicted elimination profiles shown in Fig. 4B cannot be explained by the glucuroconjugation of oxycodone, and suggest that the other metabolic pathways should be considered. For example, 6-oxycodol (produced by the 6-keto reduction) and oxycodone-*N*-oxyde (produced by flavin-containing monooxygenases) have been

Table 2
Kinetic constants (±CI95%) for oxycodone glucuronidation by human liver microsomes (HLM) and recombinant human UGTs 2B4 and 2B7.

	K_m (μM)	V_{max} (peak area/min/mg)	V_{max}/K_m
HLM	2685 ± 230	1513 ± 60	0.56
UGT2B7	762 ± 153	344 ± 20	0.45
UGT2B4	2454 ± 497	201 ± 19	0.08

Kinetic parameters were calculated by the Michaelis-Menten equation (Eq. (1)).

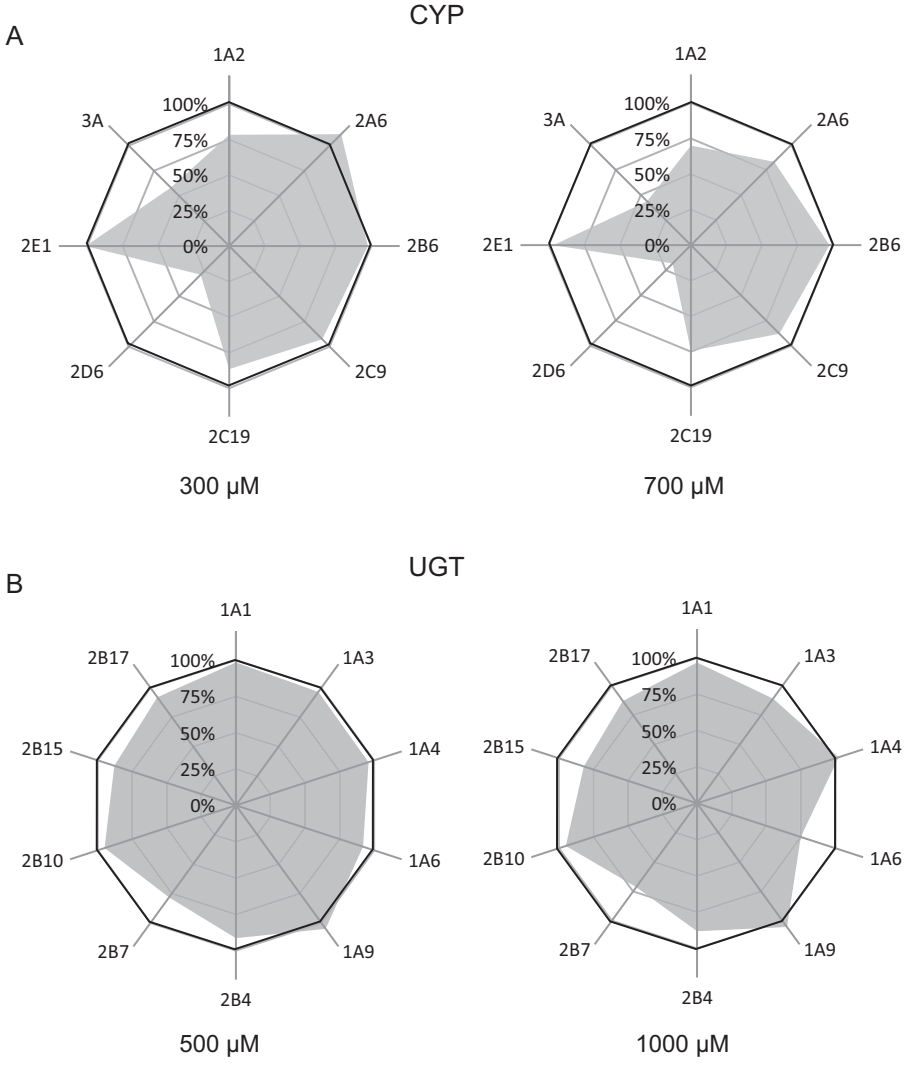

Fig. 9. Radar plot illustrating the inhibitory effects of oxycodone on (A) CYP activities using the phase I cocktail approach and (B) UGT activities using the phase II cocktail approach. The mean metabolic ratios for each oxycodone concentration are expressed as a percentage of the mean metabolic ratio obtained in the control incubation (100% of the control activity). Incubations were performed in duplicate.

Please cite this article in press as: S. Romand, et al., Characterization of oxycodone *in vitro* metabolism by human cytochromes P450 and UDP-glucuronosyltransferases, J. Pharm. Biomed. Anal. (2016), http://dx.doi.org/10.1016/j.jpba.2016.09.024

identified as oxycodone metabolites [44,45]. Moreover, sulfation represents another important route of phase II metabolism [46] and could play a role in oxycodone clearance, similar to other opioid drugs [47]. The elucidation of the main metabolic routes is an important objective for early *in vitro* metabolic studies during drug discovery, as well as the prediction of possible drug–drug interactions. Thus, the *in vitro* inhibitory properties of oxycodone were studied in the next section.

3.6. Inhibitory impact of oxycodone on microsomal CYP and UGT activities using two distinct cocktail approaches

The cocktail approach has been recently discussed as a method to drastically reduce the time and costs of the assay for *in vitro* phenotyping of drug-metabolizing enzyme activities and for studying drug–drug interactions in a single experiment [48]. A cocktail of eight specific substrates was proposed to simultaneously phenotype the eight main hepatic CYP activities in HLM [14]. In the present study, this approach was used to assess the inhibitory properties of oxycodone on the activity of the following CYP isoforms: 1A2, 2A6, 2B6, 2C9, 2C19, 2D6, 2E1 and 3A4/5. Oxycodone was incubated with the isoforms at two relatively high concentrations (*i.e.*, 300 and 700 μM) that corresponded to the *in vitro* K_m values that were previously established in the kinetic studies. As reported in Fig. 9A, at a concentration equivalent to the K_m (300 μM) of the high-affinity pathway for *O*-demethylation, oxycodone reduced the microsomal activities of the CYP2D6 and CYP3A subfamily by 72% and 42%, respectively. Whereas at 700 μM (K_m value for low-affinity pathway), oxycodone inhibited the activities of the CYP2D6 and CYP3A subfamily by 82% and 56%, respectively. These results confirmed the major involvement of the hepatic CYP2D6 and CYP3A subfamily in oxycodone metabolism. Other CYP isoforms (*e.g.*, CYP1A2 and CYP2C19) were only weakly affected by oxycodone at the highest concentration. Based on the high concentrations needed, the inhibitory properties of oxycodone could be considered as clinically irrelevant at therapeutic levels. Indeed, the *in vivo* plasma level of oxycodone was measured as 0.11 μM, corresponding to a 3000 times lower concentration than the one tested *in vitro* [11,49].

For phase II metabolism, another cocktail of ten probe substrates was incubated with oxycodone to simultaneously assess the impact of this drug on the activities of the ten main microsomal hepatic UGTs (*i.e.*, 1A1, 1A3, 1A4, 1A6, 1A9, 2B4, 2B7, 2B10, 2B15, and 2B17) [13]. The decagonal inhibition profiles (Fig. 9B) showed that when the oxycodone concentration increased, the activities of UGTs 1A3, 1A6, and all 2B subfamily decreased. Thus, oxycodone inhibited the glucuronidation activity of the aforementioned isoforms, with a stronger impact on UGT1A6 and UGT2B7. Considering the high concentrations (500 and 1000 μM) used *in vitro*, the inhibitory effect of oxycodone on phase II metabolism appears to have limited importance from a clinical point of view.

4. Conclusion

In summary, targeted inhibition studies in HLM with selective inhibitors confirmed the major involvement of CYP2D6 and CYP3A4/5 in oxymorphone and noroxycodone production, respectively. *N*-demethylation (CL_{int} of 1.46 μL/min/mg in HLM) and *O*-demethylation (CL_{int} of 0.35 μL/min/mg in human liver microsomes) were mainly involved in the elimination of oxycodone, but other metabolic pathways should be considered. The *in vitro* glucuronidation of oxycodone was studied using pooled HLM and recombinant UGTs. The isoforms 2B7 and 2B4 mainly contributed to the biotransformation of oxycodone, as confirmed by targeted inhibition studies with fluconazole and naloxone (2B4 and 2B7 selective inhibitor and 2B7-specific substrate, respectively). However, *in vitro* glucuronidation represented a very minor elimination pathway for oxycodone. Regarding the risk of drug–drug interaction evaluated using cocktail approaches, oxycodone did not exhibit significant *in vitro* inhibitory potential towards the eight monitored microsomal CYP isoforms or the ten measured microsomal UGT activities. Finally, complementary *in vitro* studies should be performed to better understand the apparent clearance of oxycodone.

Appendix A. Supplementary data

Supplementary data associated with this article can be found, in the online version, at http://dx.doi.org/10.1016/j.jpba.2016.09.024.

References

[1] M.L. Rodriguez, Oxycodone: actions, metabolism, elimination, and detection, MLO Med. Lab. Obs. 45 (2013) 24.
[2] D.P. Benziger, J. Miotto, R.P. Grandy, G.B. Thomas, R.E. Swanton, R.D. Fitzmartin, A pharmacokinetic/pharmacodynamic study of controlled-release oxycodone, J. Pain Symptom Manage. 13 (1997) 75–82.
[3] B. Lalovic, E. Kharasch, C. Hoffer, L. Risler, L.Y. Liu-Chen, D.D. Shen, Pharmacokinetics and pharmacodynamics of oral oxycodone in healthy human subjects: role of circulating active metabolites, Clin. Pharmacol. Ther. 79 (2006) 461–479.
[4] D. French, A. Wu, K. Lynch, Hydrophilic interaction LC–MS/MS analysis of opioids in urine: significance of glucuronide metabolites, Bioanalysis 3 (2011) 2603–2612.
[5] H.S. Smith, Opioid metabolism, Mayo Clin. Proc. 84 (2009) 613–624.
[6] R.C. Baselt, C.B. Stewart, Determination of oxycodone and a major matabolite in urine by electron-capture GLC, J. Anal. Toxicol. 2 (1978) 107–109.
[7] W.B. Fang, M.R. Lofwall, S.L. Walsh, D.E. Moody, Determination of oxycodone, noroxycodone and oxymorphone by high-performance liquid chromatography electrospray ionization-tandem mass spectrometry in human matrices: in vivo and in vitro applications, J. Anal. Toxicol. 37 (2013) 337–344.
[8] B. Lalovic, B. Phillips, L.L. Risler, W. Howald, D.D. Shen, Quantitative contribution of CYP2D6 and CYP3A to oxycodone metabolism in human liver and intestinal microsomes, Drug Metab. Dispos. 32 (2004) 447–454.
[9] S.V. Otton, D. Wu, R.T. Joffe, S.W. Cheung, E.M. Sellers, Inhibition by fluoxetine of cytochrome P450 2D6 activity, Clin. Pharmacol. Ther. 53 (1993) 401–409.
[10] Z.R. Chen, R.J. Irvine, A.A. Somogyi, F. Bochner, Mu receptor binding of some commonly used opioids and their metabolites, Life Sci. 48 (1991) 2165–2171.
[11] N. Marsousi, Y. Daali, S. Rudaz, L. Almond, H. Humphries, J. Desmeules, C.F. Samer, Prediction of metabolic interactions with oxycodone via CYP2D6 and CYP3A inhibition using a physiologically based pharmacokinetic model, CPT Pharmacometrics Syst. Pharmacol. 3 (2014) 1–8.
[12] H.M. Jones, K. Rowland-Yeo, Basic concepts in physiologically based pharmacokinetic modeling in drug discovery and development, CPT Pharmacometrics Syst. Pharmacol. 2 (2013) 1–12.
[13] J. Gradinaru, S. Romand, L. Geiser, P.-A. Carrupt, D. Spaggiari, S. Rudaz, Inhibition screening method of microsomal UGTs using the cocktail approach, Eur. J. Pharm. Sci. 71 (2015) 35–45.
[14] D. Spaggiari, L. Geiser, Y. Daali, S. Rudaz, Phenotyping of CYP450 in human liver microsomes using the cocktail approach, Anal. Bioanal. Chem. 406 (2014) 4875–4887.
[15] S. Romand, S. Rudaz, D. Guillarme, Separation of substrates and closely related glucuronide metabolites using various chromatographic modes, J. Chromatogr. A 1435 (2016) 54–65.
[16] G.M. Böhmer, A. Drollmann, C.H. Gleiter, R. Nave, Effect of coadministered ketoconazole a strong cytochrome P450 3A4 enzyme inhibitor, on the pharmacokinetics of ciclesonide and its active metabolite desisobutyryl-ciclesonide, Clin. Pharmacokinet. 47 (2012) 343–349.
[17] C.L. Alfaro, Y.W.F. Lam, J. Simpson, L. Ereshefsky, CYP2D6 inhibition by fluoxetine, paroxetine, sertraline, and venlafaxine in a crossover study: intraindividual variability and plasma concentration correlations, J. Clin. Pharmacol. 40 (2000) 58–66.
[18] L.A. McLaughlin, M.J.I. Paine, C.A. Kemp, J.D. Maréchal, J.U. Flanagan, C.J. Ward, M.J. Sutcliffe, G.C.K. Roberts, C.R. Wolf, Why is quinidine an inhibitor of cytochrome P450 2D6?: the role of key active-site residues in quinidine binding, J. Biol. Chem. 280 (2005) 38617–38624.
[19] C.F. Samer, Y. Daali, M. Wagner, G. Hopfgartner, C.B. Eap, M.C. Rebsamen, M.F. Rossier, D. Hochstrasser, P. Dayer, J.A. Desmeules, The effects of CYP2D6 and CYP3A activities on the pharmacokinetics of immediate release oxycodone, Br. J. Pharmacol. 160 (2010) 907–918.
[20] J.A. Williams, R. Hyland, B.C. Jones, D.A. Smith, S. Hurst, T.C. Goosen, V. Peterkin, J.R. Koup, S.E. Ball, Drug-drug interactions for UDP-glucuronosyltransferase substrates: a pharmacokinetic explanation for typically observed low exposure (AUC(i)/AUC) ratios, Drug Metab. Dispos. 32 (2004) 1201–1208.

Please cite this article in press as: S. Romand, et al., Characterization of oxycodone *in vitro* metabolism by human cytochromes P450 and UDP-glucuronosyltransferases, J. Pharm. Biomed. Anal. (2016), http://dx.doi.org/10.1016/j.jpba.2016.09.024

[21] C.T. Bedford, Glucuronic acid conjugates, J. Chromatogr. B 717 (1998) 313–326.
[22] R. Kaushik, B. Levine, W.R. LaCourse, A brief review: HPLC methods to directly detect drug glucuronides in biological matrices (Part I), Anal. Chim. Acta 556 (2006) 255–266.
[23] R.A. Ketola, K.S. Hakala, Direct analysis of glucuronides with liquid chromatography–mass spectrometric techniques and methods, Curr. Drug Metab. 11 (2010) 561–582.
[24] R. Mullangi, R.K. Bhamidipati, N.R. Srinivas, Bioanalytical aspects in characterization and quantification of glucuronide conjugates in various biological matrices, Curr. Pharm. Anal. 1 (2005) 251–264.
[25] R.M. Balliet, G. Chen, C.J. Gallagher, R.W. Dellinger, D. Sun, P. Lazarus, Characterization of UGTs active against SAHA and association between SAHA glucuronidation activity phenotype with UGT genotype, Cancer Res. 69 (2009) 2981–2989.
[26] L. Grosse, A.-S. Campeau, S. Caron, F.-A. Morin, K. Meunier, J. Trottier, P. Caron, M. Verreault, O. Barbier, Enantiomer selective glucuronidation of the non-steroidal pure anti-androgen bicalutamide by human liver and kidney: role of the human UDP-glucuronosyltransferase (UGT)1A9 enzyme, Basic Clin. Pharmacol. Toxicol. 113 (2013) 92–102.
[27] Y. Mano, T. Usui, H. Kamimura, The UDP-glucuronosyltransferase 2B7 isozyme is responsible for gemfibrozil glucuronidation in the human liver, Drug Metab. Dispos. 35 (2007) 2040–2044.
[28] H. Yamanaka, M. Nakajima, M. Katoh, A. Kanoh, O. Tamura, H. Ishibashi, T. Yokoi, Trans-3'-hydroxycotinine O- and N-glucuronidations in human liver microsomes, Drug Metab. Dispos. 33 (2005) 23–30.
[29] ACD/pKa DB, ACD/Labs Release: 12.00, Product Version: 12.01, Advanced Chemistry Development, Inc., Toronto, ON, Canada, Copyright © 1997-2009.
[30] Y. Chang, D.E. Moody, Glucuronidation of buprenorphine and norbuprenorphine by human liver microsomes and UDP-glucuronosyltransferases, Drug Metab. Lett. 3 (2009) 101–107.
[31] B.L. Coffman, C.D. King, G.R. Rios, T.R. Tephly, The glucuronidation of opioids, other xenobiotics, and androgens by human UGT2B7Y(268) and UGT2B7H(268), Drug Metab. Dispos. 26 (1998) 73–77.
[32] B.L. Coffman, G.R. Rios, C.D. King, T.R. Tephly, Human UGT2B7 catalyzes morphine glucuronidation, Drug Metab. Dispos. 25 (1997) 1–4.
[33] P. Wang, J.A. Stone, K.H. Chen, S.F. Gross, C.A. Haller, A.H.B. Wu, Incomplete recovery of prescription opioids in urine using enzymatic hydrolysis of glucuronide metabolites, J. Anal. Toxicol. 30 (2006) 570–575.
[34] V. Uchaipichat, L.K. Winner, P.I. Mackenzie, D.J. Elliot, J.A. Williams, J.O. Miners, Quantitative prediction of in vivo inhibitory interactions involving glucuronidated drugs from in vitro data: the effect of fluconazole on zidovudine glucuronidation, Br. J. Clin. Pharmacol. 61 (2006) 427–439.
[35] P. Raungrut, V. Uchaipichat, D.J. Elliot, B. Janchawee, A.A. Somogyi, J.O. Miners, In vitro-in vivo extrapolation predicts drug–drug interactions arising from inhibition of codeine glucuronidation by dextropropoxyphene, fluconazole, ketoconazole, and methadone in humans, J. Pharmacol. Exp. Ther. 334 (2010) 609–618.
[36] A. Di Marco, M. D'Antoni, S. Attaccalite, P. Carotenuto, R. Laufer, Determination of drug glucuronidation and UDP-glucuronosyltransferase selectivity using a 96-well radiometric assay, Drug Metab. Dispos. 33 (2005) 812–819.
[37] K.A. Seo, H.J. Kim, E.S. Jeong, N. Abdalla, C.-S. Choi, D.H. Kim, J.G. Shin, In vitro assay of six UDP-glucuronosyltransferase isoforms in human liver microsomes, using cocktails of probe substrates and liquid chromatography-tandem mass spectrometry, Drug Metab. Dispos. 42 (2014) 1803–1810.
[38] X. Cheng, F. Liu, T. Yan, X. Zhou, L. Wu, K. Liao, G. Wang, H. Hao, Metabolic profile, enzyme kinetics, and reaction phenotyping of beta-lapachone metabolism in human liver and intestine in vitro, Mol. Pharm. 9 (2012) 3476–3485.
[39] M.T. Donato, N. Jiménez, J.V. Castell, M.J. Gómez-Lechón, Fluorescence-based assays for screening nine cytochrome P450 (P450) activities in intact cells expressing individual human P450 enzymes, Drug Metab. Dispos. 32 (2004) 699–706.
[40] J. Joo, B. Lee, T. Lee, K.H. Liu, Screening of six UGT enzyme activities in human liver microsomes using liquid chromatography/triple quadrupole mass spectrometry, Rapid Commun. Mass Spectrom. 28 (2014) 2405–2414.
[41] E.J. Cone, R. Heltsley, D.L. Black, J.M. Mitchell, C.P. LoDico, R.R. Flegel, Prescription opioids. I. Metabolism and excretion patterns of oxycodone in urine following controlled single dose administration, J. Anal. Toxicol. 37 (2013) 255–264.
[42] R. Poyhia, T. Seppala, K.T. Olkkola, E. Kalso, The pharmacokinetics and metabolism of oxycodone after intramuscular and oral-administration to healthy-subjects, Br. J. Clin. Pharmacol. 33 (1992) 617–621.
[43] D.A. Yee, B.M. Best, R.S. Atayee, A.J. Pesce, Observations on the urine metabolic ratio of oxymorphone to oxycodone in pain patients, J. Anal. Toxicol. 36 (2012) 232–238.
[44] A. Baldacci, J. Caslavska, A.B. Wey, W. Thormann, Identification of new oxycodone metabolites in human urine by capillary electrophoresis-multiple-stage ion-trap mass spectrometry, J. Chromatogr. A 1051 (2004) 273–282.
[45] T. Ishida, K. Oguri, H. Yoshimura, Isolation and identification of urinary metabolites of oxycodone in rabbits, Drug Metab. Dispos. 7 (1979) 162–165.
[46] N. Gamage, A. Barnett, N. Hempel, R.G. Duggleby, K.F. Windmill, J.L. Martin, M.E. McManus, Human sulfotransferases and their role in chemical metabolism, Toxicol. Sci. 90 (2006) 5–22.
[47] K. Kurogi, A. Chepak, M.T. Hanrahan, M.-Y. Liu, Y. Sakakibara, M. Suiko, M.-C. Liu, Sulfation of opioid drugs by human cytosolic sulfotransferases: metabolic labeling study and enzymatic analysis, Eur. J. Pharm. Sci. 62 (2014) 40–48.
[48] D. Spaggiari, L. Geiser, Y. Daali, S. Rudaz, A cocktail approach for assessing the in vitro activity of human cytochrome P450s: an overview of current methodologies, J. Pharm. Biomed. Anal. 101 (2014) 221–237.
[49] C.F. Samer, K.I. Lorenzini, V. Rollason, Y. Daali, J.A. Desmeules, Applications of CYP450 testing in the clinical setting, Mol. Diagn. Ther. 17 (2013) 165–184.

Please cite this article in press as: S. Romand, et al., Characterization of oxycodone *in vitro* metabolism by human cytochromes P450 and UDP-glucuronosyltransferases, J. Pharm. Biomed. Anal. (2016), http://dx.doi.org/10.1016/j.jpba.2016.09.024